Journal of the Korean Crystal Growth and Crystal Technology
Vol. 20, No. 5 (2010) 202-206

Growth parameters and formation of slip plane in $ZnWO_4$ single crystals by the Czochralski method

Chang Sung Lim†

Department of Advanced Materials Science & Engineering, Hanseo University, Seosan 356-706, Korea

(Received September 17, 2010)
(Revised October 11, 2010)
(Accepted October 12, 2010)

Abstract Single crystals of $ZnWO_4$ were grown successfully in the [100], [010] and [001] directions using the Czochralski method. The growth parameters and the formation of slip plane in $ZnWO_4$ crystals were studied. $ZnWO_4$ crystals had a cleavage plane of (010). The dislocation density on the (010) plane at the center of the crystal was lower than that of the edge region. It was inferred that the high density at the edge of the crystals was caused by the thermal gradient during crystal growth. The etch pit arrangement revealed the (100) slip plane to be most active during crystal growth.

Key words Growth parameters, Slip plane, $ZnWO_4$, Czochralski method

1. Introduction

$ZnWO_4$ is one of the most important inorganic materials, which has the monoclinic wolframite-type structure with the space group P2/c. There are two formula units per primitive cell with lattice parameters of a = 4.69263 Å, b = 5.72129 Å, c = 4.92805 Å and β = 90.6321° [1]. In recent years, $ZnWO_4$ has attracted considerable attention for potential applications as a scintillator, maser, luminescent material and photocatalyst [2-7]. The physical, chemical and photochemical properties of $ZnWO_4$ were dependent on the manufacturing method. To enhance the applications of $ZnWO_4$, several processes have been developed over the last decade. $ZnWO_4$ is prepared by processes, such as solid-state reaction method [8], co-precipitation method [9], molten salt [10], combustion [11], mechano-chemical [12] sol-gel [13], hydrothermal reaction [14-16].

For high quality applications, $ZnWO_4$ single crystals are generally grown by the Czochralski method [7, 17-19]. However, the crystal growth mechanisms of $ZnWO_4$ are complicated and are still a challenge for commercial applications. Therefore, for improved applications, a more detailed study of the growth parameters and characteristics of $ZnWO_4$ single crystals by the Czochralski method are needed.

In this study, single crystals of $ZnWO_4$ in the [100], [010] and [001] directions were grown successfully by the Czochralski method. The growth parameters in the [100], [010] and [001] directions were examined as the function of the rotation speed, pulling rate and diameter of the grown crystals. Subsequently, the formation of slip plane in $ZnWO_4$ crystals were studied in detail.

†Corresponding author
Tel: +82-41-660-1445
Fax: +82-41-660-1445
E-mail: cslim@hanseo.ac.kr

2. Experimental Procedure

The equipment for the Czochralski method was fabricated using a furnace assembly. The $ZnWO_4$ melts were prepared from polycrystalline $ZnWO_4$, placed in a platinum crucible. The platinum crucible was heated in a furnace fabricated with SiC resistive heating elements, and the temperature was monitored and regulated using a controller and thyrister(Eurotherm Co.). The polycrystalline $ZnWO_4$ was prepared from stoichiometric amount of the mole ratio of 1 : 1 for zinc oxide and tungsten trioxide. The mixed powders was pressed and calcined at 800, 900, 1000 and 1100°C for various times.

The single crystals were pulled along the crystallographic axes with a diameter of 0~3.5 cm at pulling rate of 0~100 mm/h and a rotation speed of 0~68 rpm. The temperatures were controlled precisely with the measurements on the surface of the $ZnWO_4$ melts between 1230~1235°C during growth. The rotation speed was fixed to 40 rpm, and the pulling rate was 0~10 mm/h. The maximum diameter was 1.9 mm and the crystal had a red-brown color. Seed crystals were fabricated with a length and diameter of 2.5 cm and 0.2 cm, respectively,

Table 1
Typical growth procedure and parameters of the grown $ZnWO_4$ single crystals

Parameter procedure	Temperature (°C)	Pulling rate (mm/h)	Rotation speed (rpm)
Melting	1235	0	60
Dipping	1233	5	60
Necking	1234	8	60
Crowning	1231	3.5	60
Growing	1230	8~10	60
Tailing	1233	10	60

and employed for crystal growth along the crystallographic direction after identifying the crystal orientation by Laue back reflection. The $ZnWO_4$ single crystals were grown using the typical growth procedure and parameters listed in Table 1. The temperature was controlled between 1230~1235°C, the rotation speed was fixed to 60 rpm and the pulling rate was between 0~10 mm/h.

The microstructure of the etch pits were observed by optical microscopy. The dislocations in the cleaved slices were examined by chemical etching. The etched surfaces were obtained from the boiling a 2 molar NaOH solution. The (010) surface was etched in a boiling solution for 4 min, whereas the (001) and (100) surfaces were etched for 2 min. The orientations of $ZnWO_4$ single crystals in [100], [010] and [001] directions were identified from the Laue back reflection patterns.

3. Results and Discussion

For the Czochralski growth of single crystals with a specific orientation, a seed crystal was fixed properly to the pulling rod. Platinum wires were used to obtain seed crystals employing the capillary action from the melt. The platinum wires were dipped into the melt and the temperature was adjusted, a small crystal was grown inside the hole of the four platinum wires by capillary action. The temperature at the hole of the platinum wires was lower than the surface of the melt, so that nucleation occurred at a lower temperature. This crystal consisted of two crystals, due to heteronucleation during the dipping procedure at a lower temperature.

The grown crystals showed perfect cleavage in the (010) plane, and the thin sections were found to cleave along the (101) plane. The (100) twin appeared to be the most common along the (101) plane. Fig. 1 shows the grown single crystals of $ZnWO_4$ in the [100], [010] and [001] directions, which corresponds to Table 2 (A), (B), (C) with the growth direction, rotation speed and diameter. As listed in Table 2, the rotation speed was between 40~54 rpm with a diameter of 20 mm for the [100] direction in Fig. 1(a), whereas it was 46 rpm with a diameter of 17 mm for the [101] direction in Fig. 1(b) and 63 rpm with a diameter 23 mm for the [001] direction in Fig. 1(c). The formation of cracking in the grown crystals in [001] direction during the cooling process can be prevented by annealing at 800°C for 10 h.

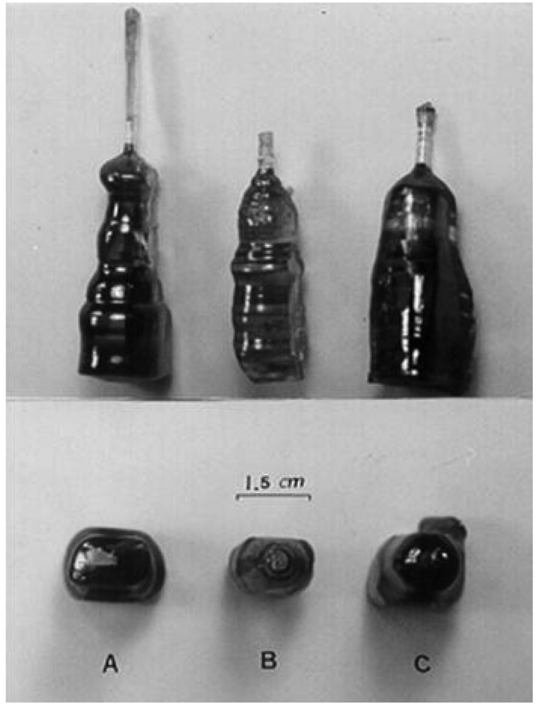

(a) (b) (c)

Fig. 1. The grown single crystals of $ZnWO_4$ in (a) [100], (b) [010] and (c) [001], which corresponds to Table 2 (A), (B) and (C) with the growth direction, rotation speed and diameter.

Table 2
Growth conditions of the grown $ZnWO_4$ single crystals of (A) [100], (B) [010] and (C) [001]

Crystals / Conditions	A	B	C
Direction	[100]	[010]	[001]
Rotation speed (rpm)	54, 40	46	63
Weight (g)	85.9	47.0	90.7
Annealing effect	no	800°C, 10 h	800°C, 10 h
Remark	crack	bubble	no crack no bubble

*The crystal data of A, B, C are corresponding to the crystal in Fig. 1(a), (b), (c).

Fig. 2 shows the structure of the $ZnWO_4$ single crystal. It is based on a distorted hexagonal close packing of O atoms with Zn and W atoms, each occupying one-fourth of the octahedral interstices. The presence of two

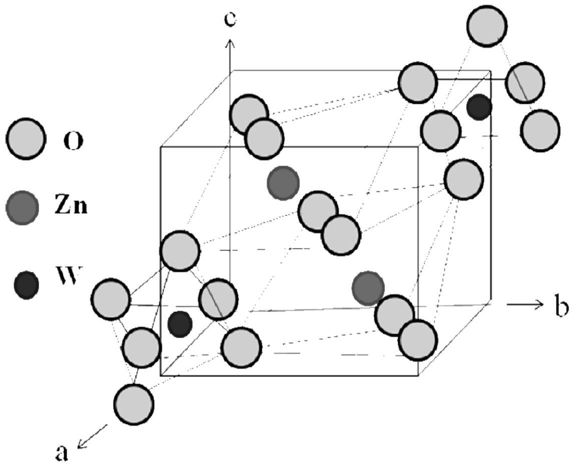

Fig. 2. The structure of the $ZnWO_4$ single crystal. Each chain of the ZnO_6 octahedra is corner-linked, and the chains of the WO_6 octahedra are edge-linked, which are also parallel to [001].

non-equivalent oxygen atoms is responsible for the pairs of Zn-O and W-O bonds with different lengths. Therefore, both Zn and W atoms are surrounded by six oxygen atoms, forming distorted octahedral coordination. Each chain of the ZnO_6 octahedra is corner-linked, and the chains of WO_6 octahedra are edge-linked, which are also parallel to [001]. The ZnO_6 and WO_6 octahedra consist of three pairs of cation-oxygen bonds with Zn and W atoms being displaced from the center of their octahedra by approximately 0.29 and 0.32 Å, respectively, along the [010] direction [9]. Since two similar atoms in a unit cell are related by a center of symmetry, they are off center in the opposite sense in a manner characteristic of an antiferroelectric.

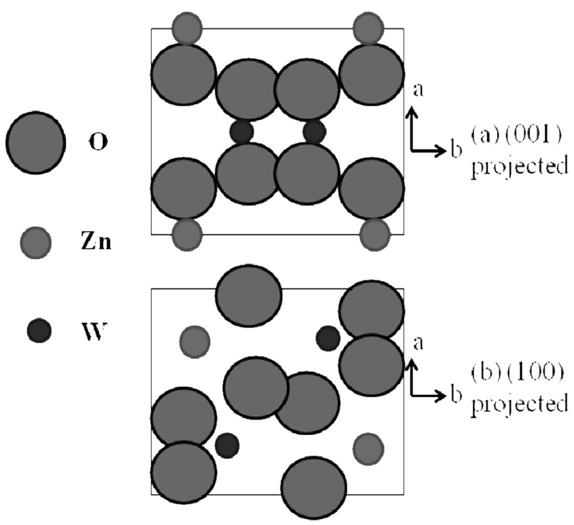

Fig. 3. The unit cell of $ZnWO_4$ projected on the (001) and (100) plane.

Fig. 3 shows the unit cell of $ZnWO_4$ projected on the (001) and (100) plane. For the (100) planes the oxygen atoms are halfway between the reflecting planes, and are located in the region of maximum field amplitude of the anomalously transmitted standing wave. Therefore, oxygen atoms absorb the transmitted wave. However, for (001) planes, oxygen atoms are displaced from the position of the maximum field amplitude, which means that they absorb less than the (100) reflection. Therefore, the intensity of the (001) reflection is approximately 2 to 3 times that of the (100) reflection. This difference in intensity is due to the different locations of the oxygen atoms relative to the position of the maximum field amplitude in the two reflections.

The dislocation density of $ZnWO_4$ was obtained from the etch pits of the surface of the grown crystals. Fig. 4 shows the etch patterns of (010) plane of the grown $ZnWO_4$ single crystals. The dislocation density at the center of the crystal was lower than that of the edge of the crystal. The features of the dislocations of the (010) plane were propagated along the [001] direction. The etch pit arrangement shows that slip occurred along the (100) plane, particularly near the edge of the crystal. It is possible that a dislocation of this type grew or slipped on either the (010) or (100) slip planes. The straight dislocations near the center of the crystal would suggest that extensive cross slip had occurred in the crystal.

When slip in the (100) plane is concentrated in a slip band, as indicated by the presence of etch pits on the adjacent section in Fig. 4, dislocations appear in all anomalous transmission reflections. This probably occurs because the strain fields of the dislocations superpose and the edge components of these dislocations are slightly visi-

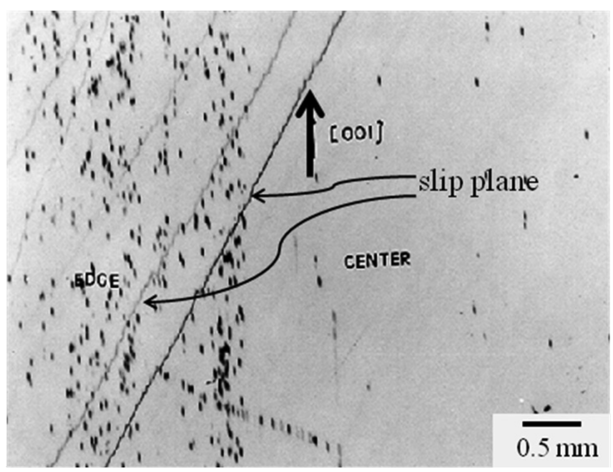

Fig. 4. Etch patterns of the (010) plane of the grown $ZnWO_4$ single crystals.

ble in any plane not perpendicular to them. The etch pits were similar for all crystals grown in the [001], [010], [100] directions. When a crystal is grown in the [001] direction, as is usual for maser applications, the (100) and (010) slip planes are parallel to the growth direction. Existing dislocations, either in the seed or generated in the crystal, can slip, intersect the solid-liquid interface, and then continue to propagate by growth. These arrays coincide with the low-angle grain boundaries, whose tilt could be observed under a microscope.

The crystallographic orientation of $ZnWO_4$ crystal could be also considered. $ZnWO_4$ has a monoclinic wolframite structure in the space group P2/c. There are two formula units per primitive cell with the lattice parameters a = 4.69263 Å, b = 5.72129 Å, c = 4.92805 Å and β = 90.6321°. Cleavage gives a (010) crystal face, and etching gives rise to etch pits aligned parallel to the (100) slip plane in the [001] direction. The optic plane in $ZnWO_4$ is perpendicular to the (010) cleavage plane. The lattice parameter of b (5.72129 Å) is longer than that of a (4.69263 Å) and c (4.92805 Å). Hence, the cleavage surface propagates on the (010) plane.

4. Conclusions

Single crystals of $ZnWO_4$ were grown successfully in the [100], [010] and [001] directions by the Czochralski method. The seed crystals of $ZnWO_4$ were obtained from single crystal growth on platinum wires due to capillary action from the melt. The rotation speed was controlled between 40~54 rpm with a diameter of 20 mm for the [100] direction, whereas the speed was 46 rpm with a diameter of 17 mm for the [101] direction and 63 rpm with a diameter 23 mm for the [001] direction. The $ZnWO_4$ crystals had a cleavage plane of (010). The dislocation density on the (010) plane at the center of the crystal was lower than that of the edge. The higher dislocation density at the edge of the crystals was attributed to the thermal gradients of the growing crystals. The etch pit arrangement shows that the (100) slip plane appeared to be most active during crystal growth.

Acknowledgement

This research was supported by Basic Science Research Program through the National Research Foundation of Korea(NRF) funded by the Ministry of Education, Science and Technology (2010-0023911).

References

[1] A. Kalinko, A. Kuzmin and R.A. Evarestov, "Ab initio study of the electronic and atomic structure of the wolframite-type $ZnWO_4$", Solid State Comm. 149 (2009) 425.

[2] P. Belli, R. Bernabei, F. Cappella, R. Cerulli and F.A. Danevich, "Search for double beta decay of zinc and tungsten with low background $ZnWO_4$ crystal scintillators", Nuc. Phys. A826 (2009) 256.

[3] X. Cao, W. Wu, N. Chen, Y. Peng and Y. Liu, "An ether sensor utilizing cataluminescence on nanosized $ZnWO_4$", Sensors and Actuators B137 (2009) 83.

[4] C. Yu and J.C. Yu, "Sonochemical fabrication, characterization and photocatalytic properties of $Ag/ZnWO_4$ nanorod catalyst", Mat. Sci. Eng. B 164 (2009) 16.

[5] S. Lin, J. Chen, X. Weng, L. Yang and X. Chen, "Fabrication and photocatalysis of mesoporous $ZnWO_4$ with PAMAM as a template", Mat. Res. Bull. 44 (2009) 1102.

[6] M. Itoh, T. Katagiri, T. Aoki and M. Fujita, "Photostimulated luminescence and photo-induced infrared absorption in $ZnWO_4$", Radiation Measurements 42 (2007) 545.

[7] V. Nagirnyi, L. Jonsson, M. Kirm, A. Kotlov, A. Lushchik, I. Martinson, A. Watterich and B.I. Zadneprovski, "Luminescence study of pure and Fe- or Mo-doped $ZnWO_4$ crystals", ibid. 38 (2004) 519.

[8] G.B. Kumar, K. Sivaiah and S. Buddhudu, "Synthesis and characterization of $ZnWO_4$ ceramic powder", Cer. Int. 36 (2010) 199.

[9] X.G. Huang and Y. Zhu, "Synthesis and photocataytic performance of $ZnWO_4$ catalyst", Mat. Sci. Eng. B 139 (2007) 201.

[10] X. Jiang, J. Ma, J. Liu, Y. Ren, B. Lim, J. Tao and X. Zhu, "Synthesis of $ZnWO_4$ nano-particles by a molten salt method", Materials Letters 61 (2007) 4595.

[11] T. Dong, Z. Li, Z. Ding, L. Wu, X. Wang and X. Fu, "Characterization and properties of Eu^{3+}-doped $ZnWO_4$ prepared via a facile self-propagating combustion method", Mat. Res. Bull. 43 (2008) 1694.

[12] A. Dodd, A. Mckinley, T. Tsuzuki and M. Saunders, "Mechanochemical synthesis of nanoparticulate ZnO-$ZnWO_4$ powders and their photocatalytic activity", J. Euro. Cer. Soc. 29 (2009) 139.

[13] X. Zhao, W. Yao, Y. Wu, S. Zhang. H. Yang and Y. Zhu, "Fabrication and photo-electrochemical properties of porous $ZnWO_4$ film", J. Sol. Stat. Che. 179 (2006) 2562.

[14] F.-S. Wen, X. Zhao, H. Huo, J.-S. Chen, E. Shu-Lin and J.-H. Zhang, "Hydrothermal synthesis and photoluminescent properties of $ZnWO_4$ and Eu^{3+}-doped $ZnWO_4$", Mat. Lett. 55 (2002) 152.

[15] G. Huang, C. Zhang and Y. Zhu, "$ZnWO_4$ photocatalyst with high activity for degradation of organic contaminants", J. Alloys and Compounds 432 (2007) 269.

[16] H. Fu, J. Lin, L. Zhang and Y. Zhu, "Photocatalytic activities of a novel $ZnWO_4$ catalyst prepared by a hydrothermal process", Applied Catalysis A: General 306 (2006) 58.

[17] A. Kornylo, A. Jankowska-Frydel, B. Kuklinski, M.

Grinberg, N. Kruyiak, Z. Moroz and M. Pashkowsky, "Growth and spectroscopy of Ni^{2+} in $ZnWO_4$ crystal", Radiation Measurement 38 (2004) 707.
[18] L. Malicsko, A. Peter and W. Erfurth, "Spectroscopic properties of single crystal doped with Fe and Li impurities", J. Crystal Growth 151 (1995) 127.
[19] L. Malicsko, A. Peter and W. Erfurth, "Characterization of $ZnWO_4$: Fe single crystals by optical and scanning electron microscopic methods", ibid. 151 (1995) 127.